CHEMICAL ENGINEERING TRANSACTIONS
VOL. 31, 2013
A publication of AIDIC
The Italian Association of Chemical Engineering
Online at: www.aidic.it/cet
Guest Editors: Eddy De Rademaeker, Bruno Fabiano, Simberto Senni Buratti

ISBN 978-88-95608-22-8; **ISSN** 1974-9791
DOI: 10.3303/CET1331134

Lattice Boltzmann Method: A New Alternative for Loss Estimation

Juan C. Díaz Cruz*[a], Sergio E. Rodríguez[a], Sergio A. Ordóñez[b], Felipe Muñoz[a]
[a]Chemical Engineering Department, Universidad de los Andes, Bogotá, Colombia
[b]Singapore-ETH Centre, Future Cities Laboratory
jc.diaz111@uniandes.edu.co

In order to estimate primary containment losses in the industry, two methods have been traditionally used: Source Models (SM) and conventional Computational Fluid Dynamics models (CFD). However, these methods have some disadvantages in terms of accuracy for the former and calculation time for the latter, making the analysis of losses inefficient. In an attempt to overcome these disadvantages, this work proposes the use of the Lattice Boltzmann method (LBM) to perform free surface simulations over loss of primary containment (LOC) scenarios. The LBM was written in C++ and the scenarios were modelled and validated through the comparison with experimental and specialized software data (FLUENT-ANSYS). It was possible to verify that the difference in simulation time between FLUENT-ANSYS and LBM increases as the grid resolution increases. Moreover, this work proves that both computational methods predict correctly the studied phenomenon. Hence, the LBM is suggested as an alternative to estimate primary containment losses, being especially attractive in complex geometry simulations that require high grid resolution.

1. Introduction

Storage vessels, pipes and chemical reactors are some examples of units inside a chemical industrial facility that can lead to the release of toxic or dangerous materials. An accurate prediction of the material release is fundamental for proper risk assessments and consequence estimation. To accomplish this, it is essential to determine factors such as the amount of material available, the emission time, the rate of release and the material's phase. Two methods are commonly used for the estimation of material release: Source Models (SM) and Computational Fluid Dynamics methods (CFD).

SM are typically adequate for rapid calculations and are based on empirical or simplified physical equations (Crowl and Louvar, 2002). SM strongly rely on specific parameters, which are usually unknown prior to the incident, implying high uncertainty on the results obtained. On the other hand, conventional CFD can be used; this approach is able to simulate fluid flow by the numerical solution of the Navier-Stokes (NS) conservation equations (Ferziger and Peric, 2002). The CFD approach, unlike SM, allows the inclusion of specific elements in the simulations such as obstacles and atmospheric conditions (Pontiggia et al., 2012); for this reason, CFD analysis provides more accurate and realistic results. However, this method requires an additional model for the simulation of free surfaces (e.g VOF for FLUENT), which often leads to increased computational costs.

As a way to overcome the issues mentioned above, this study poses the simulation of a Newtonian liquid release by the use of the Lattice Boltzmann Method (LBM), analysing the LOC scenario and the pool formation process. The LBM is a model used to simulate fluid flow based on the solution of the Boltzmann equation adjusted for modelling the NS conservation equations (Succi, 2001). Unlike the SM and conventional CFD methods, this alternative allows including obstacles in the simulations with complex and detailed geometries without significantly affecting the computational performance. In addition, the LBM has several computational advantages over the conventional CFD models; for example, parallelizing the process can easily and substantially reduce the computation time.

2. The Lattice Boltzmann Method (LBM)

It has been demonstrated that the LBM, is an effective numerical solver (Succi, 2001). The method has been successfully applied to various hydrodynamic problems with excellent results (Sukop and Throne, 2006). It is considered as an alternative to model fluid motion without solving directly the Navier-Stokes and continuity

Please cite this article as: Diaz Cruz J., Rodríguez S.E., Ordonez S. and Munoz F.G., 2013, Lattice boltzmann method: new alternative for loss estimation, Chemical Engineering Transactions, 31, 799-804 DOI: 10.3303/CET1331134

equations. The LBM focuses on the modelling of streaming and collision processes at each time step, discretizing space, time and velocities, and introducing a collision process based in Chapman-Enskog's expansions from the Navier-Stokes equation (Skordos, 1993).
In the LBM a fluid is described in terms of a density distribution functions $f(r,t)$, which give the probability of finding a fictitious particle in a lattice r with velocity v (Succi, 2001). Each cell has Q discretized velocity directions, depending on the implemented model. For the Bhatnagar-Gross-Krook (BGK) model together with $D2Q9$, every particle has 9 possible directions to move across the e_i vectors (As shown in Table 1).

Table 1. Discrete velocities.

Vector $\boldsymbol{e_i}$	$(\mathbf{0},\mathbf{0})$	$\left(\boldsymbol{cos}\left[(\boldsymbol{i}-\mathbf{1})\frac{\boldsymbol{\pi}}{\mathbf{4}}\right],\boldsymbol{sin}\left[(\boldsymbol{i}-\mathbf{1})\frac{\boldsymbol{\pi}}{\mathbf{4}}\right]\right)\boldsymbol{c}$	$\left(\boldsymbol{cos}\left[(\boldsymbol{i}-\mathbf{1})\frac{\boldsymbol{\pi}}{\mathbf{4}}\right],\boldsymbol{sin}\left[(\boldsymbol{i}-\mathbf{1})\frac{\boldsymbol{\pi}}{\mathbf{4}}\right]\right)\sqrt{\mathbf{2}}\boldsymbol{c}$
Velocity i	$i=0$	$i=1,3,5,7$	$i=2,4,6,8$

Equation 1 describes the distribution function dynamics in BGK, where Δt is the time step of the simulation, τ is the relaxation parameter, Ω the term associated with particle collision and f_i^{eq} is the local equilibrium function which is determined in the Equation 2.

$$f_i(x+e_i\Delta t, t+\Delta t) = f_i(x,t) + \Omega_i \,, where\ \Omega_i = -\frac{1}{\tau}\left[f_i\,(x,t) - f_i^{eq}\,(x,t)\right] \tag{1}$$

$$f_i^{eq}(x) = \omega_i \rho(x)\left[1 + 3\frac{e_i\cdot u}{c^2} + \frac{9}{2}\frac{(e_i\cdot u)^2}{c^4} - \frac{3}{2}\frac{u^2}{c^2}\right] \tag{2}$$

Where ω_i is a weighting factor explained in (Sukop and Throne, 2006).
When the distribution functions are known, it is possible to determine the fluid's macroscopic properties such as density, velocity and the stress tensor using the Equation set 3, respectively:

$$\rho = \sum_{i=0}^{8} f_i \qquad u = \frac{1}{\rho}\sum_{i=0}^{8} f_i\, e_i \qquad \Pi_{\alpha\beta} = \sum_i e_{i\alpha} e_{i\beta}\left(f_i - f_i^{eq}\right) \tag{3}$$

On the other hand, the BGK equation makes it possible to determine the dynamic viscosity and pressure as described in the Equation set 4.

$$\mu = \frac{\rho}{3}\left(\tau - \frac{1}{2}\right) \qquad P = c_s^2\rho \tag{4}$$

For treatment of boundary conditions see: (Chang et al., 2009, Lee and Lee, 2010, Yang, 2010, Maier et al., 1996).

3. Free Surface simulations with LBM

Unlike the basic LBM which has only one cell type (fluid), the free surface model requires three cells types: gas phase, interface (partly filled) and fluid cells (Thürey, 2007). Gas cells do not have fluid; this means that they do not have distribution functions. For this reason, these cells cannot stream distribution functions to interface cells; as a consequence, interface cells must reconstruct their distribution function set after each streaming step. This can be achieved by recalculating the empty distribution functions using the previous time velocity and density information of the interface cell; Equation 5 is used for this process.

$$f_i(x, t+\Delta t) = f_i^{eq}(\rho_a, u) + f_{\bar{i}}^{eq}(\rho_a, u) - f_i(x,t) \tag{5}$$

Here ρ_a is related with atmospheric pressure and is equal to one according to Thürey's algorithm, $f_{\bar{i}}$ is the distribution function opposite to f_i. Afterwards, it is necessary to track the fluid's mass in each interface cell; this can be calculated using Equation 6.

$$m(x, t+\Delta t) = m(x,t) + \sum_i \frac{\epsilon(x+e_i\Delta t, t) + \epsilon(x,t)}{2}\left(f_{\bar{i}}(x+e_i\Delta t, t) - f_i(x,t)\right) \tag{6}$$

Here ϵ is the filled fraction of the cell calculated as $\epsilon = m/\rho$.
After the two calculations explained above, all the interface cells have a complete distribution function set and the mass is conserved. Now, the collision step is ready to be performed. After it, the interface cell type must be updated according to its new type. To ensure continuity on the interface layer, some fluid or gas cells must be converted into interface cells. To see the details of this algorithm it is advisable to review (Thürey, 2007).

4. Methodology

This work is based on a case study relevant to process safety: liquid spills due to LOC. This type of simulation is naturally on transient state; furthermore, it is necessary to incorporate free surface models because the control volume of the system is made up by liquid and air. The LBM explained by (Sukop and Throne, 2006) was implemented with the free surface model proposed by (Körner et al., 2005) and (Thürey, 2007). The implemented methods were programmed in C++ and OpenGL+GLUT libraries were used to create solution animations in order to validate the model against laboratory assays of fluid spills. Finally, a comparison between conventional CFD, LBM and experimental data was made to determine the computational efficiency and quality of the results from each method.

4.1. Case Study

The LOC of a tank filled with cm^3 of glycerin was studied. As the tank is emptied, the released liquid falls inside a bigger tank. The small tank is a rectangular prism with a cm cm base and a cm height. The released liquid flows through a cm tall and cm deep orifice. Figure 1 illustrates the system. The whole study was performed on a lateral perspective (XY plane), therefore all simulations are in 2D.

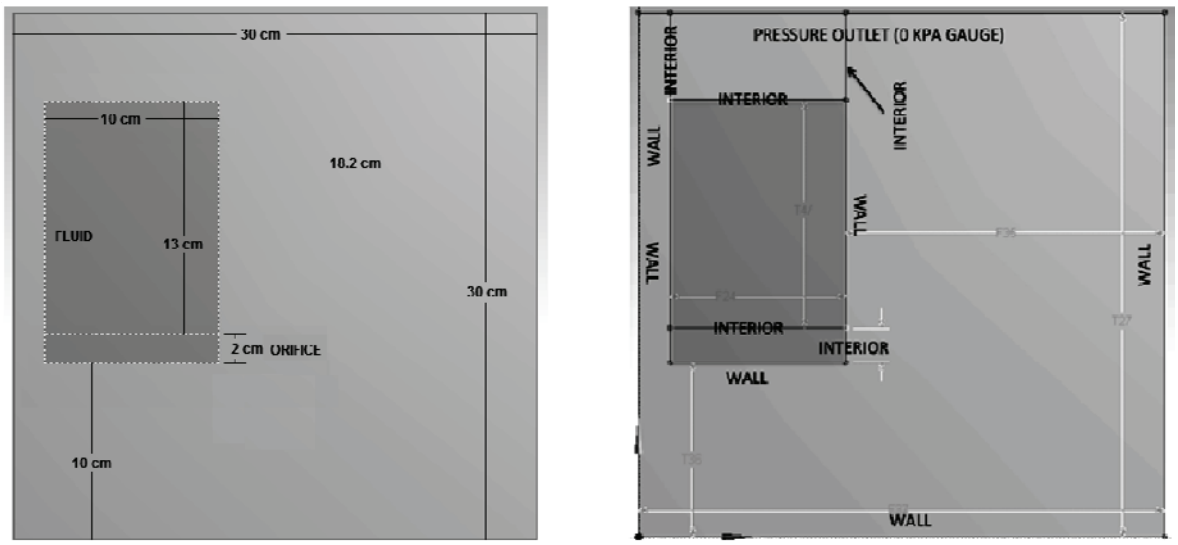

Figure 1: Left: Case study diagram, Right: Boundary conditions for FLUENT.

4.2. LBM Simulations

The geometry described in Figure 1 was programmed into the LBM code and the following simulation conditions were established: (i) Grid resolution: , (ii) cell size: m/cell, (iii) time step: s/click, (iv) kinematic viscosity: m^2/s, (v) bounce back boundary condition in walls (He et al., 1997), (vi) gravitational field action. For each simulation, the execution time was registered and an animation was generated for further image analysis.

4.3. FLUENT simulations

The geometry described in Figure 1 was build using ANSYS Design Modeler. In order to make a comparison as fair as possible and to ensure that both methods solve the same number of elements, the mesh in FLUENT was made up by orthogonal square elements to recreate the LBM grid. The solution methods and the boundary conditions used in these simulations are shown in Table 2 and Figure 1 (Right) respectively.

Table 2: Solution methods for FLUENT.

Pressure and Velocity Coupling		PISO
Spatial Discretization	Gradient	Green-Gauss Cell Based
	Pressure	PRESTO!
	Momentum	Second Order Upwind
	Volume Fraction	Geo-Reconstruct
Transient Formulation		First Order Implicit

4.4. Experimental Procedure

Two acrylic containers were installed according to the measures shown in Figure 1. 1500 cm^3 of glycerin were stained with 0.4 g of rhodamine in order to increase image contrast and facilitate the post-processing of information. The liquid release process was recorded at 500 frames per second using a Photron Fastcam 1024 PCI camera. After that, each frame was analysed using a MATLAB image processing routine.

4.5. Image Analysis

The objective of the image analysis is to track the jet's length in time during the release process; this length was measured relative to a reference point located 4 cm under the tank's orifice. This tracking process was performed over the three models: LBM, FLUENT and experimental data. For all models, the jet's length was measured at each frame using MATLAB's image processing tools. The time elapsed since the beginning of the spill was defined by the image recording speed of the simulations or the camera.

4.6. Performance comparison between computational methods

Several simulations were performed using the same geometry but varying the number of elements in the mesh. For each of these simulations, the time taken by both methods to simulate 1 real second of the spill was measured. It must be noted that time steps on both methods are not directly comparable due to the fact that typically a time step in FLUENT takes much more computing time than one using the LBM; but on the other hand, FLUENT is able to tolerate much bigger steps (Thürey, 2007). That's why a comparison system based on real time rather than on time steps was chosen. The different grid resolutions used are shown in Table 3. All simulations were executed on the same computer (Windows 7, Intel Xenon 2.67GHz (x12), 48 GB RAM).

Table 3: Grid resolutions used for simulation time comparisons.

Simulation No.		1	2	3	4	5	6	7	8	9
FSLBM	**Elements**	3600	10000	25600	40000	67600	90000	160000	250000	1000000
FUENT (VOF)	**Elements**	2524	6400	10080	25605	40052	62528	160168	-	-

5. Results and Discussion

All LBM simulations mentioned in this section were performed using a C++ program developed from scratch by the authors.

5.1. Computing time

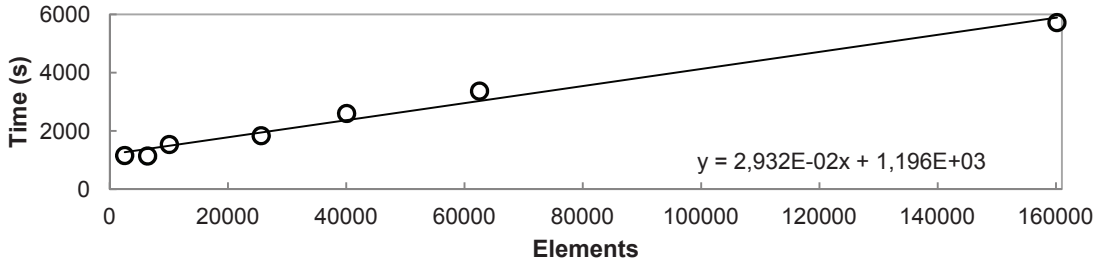

Figure 2: Performance plot for FLUENT (VOF).

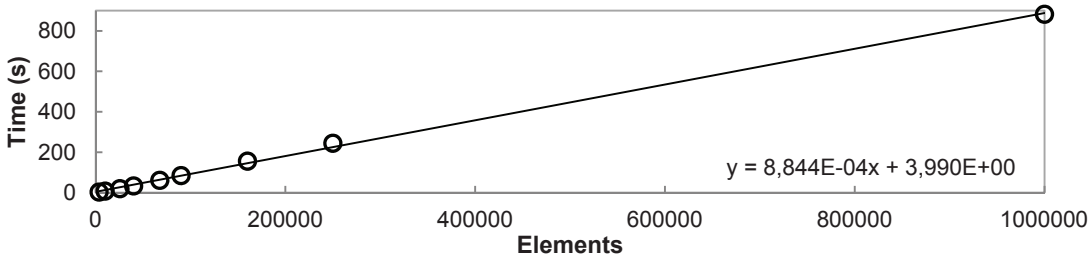

Figure 3: Performance plot for LBM.

Both methods exhibit a linear relation between the computing time and the number of elements in the studied range (Figures 2 and 3). The performance plot slopes for LBM and FLUENT are $8.844 * 10^{-4}$ and $2.932 * 10^{-2}$ seconds/element (respectively). With this information, it is possible to conclude that: (i) For a same number of

elements, LBM will always be faster than FLUENT, (ii) simulation time grows faster in FLUENT simulations than in LBM simulations as the number of elements increases, (iii) the difference in computing time between both methods increases as the number of elements increases.

5.2. Flow pattern

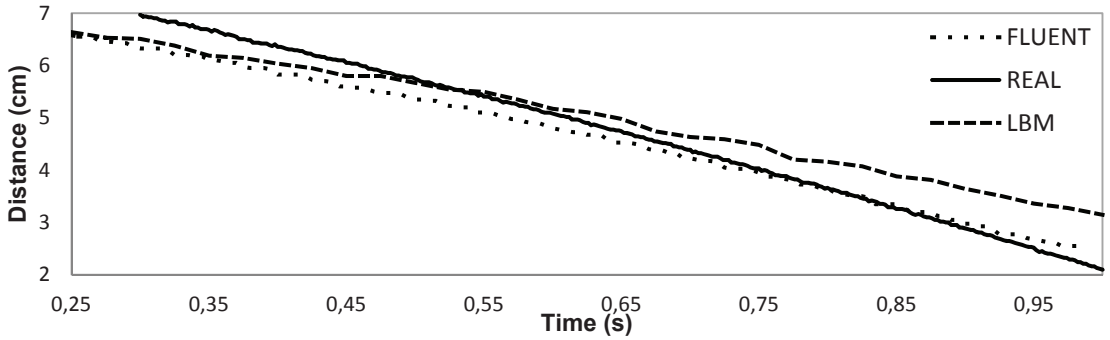

Figure 4: Jet's length versus time for the three studied methods.

The experimental data reported in Figure 4 shows that there is a linear relation between the jet's length and time regarding the flow dynamics in this scenario; this same behaviour is observed in FLUENT and LBM simulations. This suggests the following: (i) LBM approximates correctly the fluid velocity and pressure fields, (ii) LBM simulates correctly the flow dynamics under the presence of body forces like gravity, (iii) The unit conversion method between LBM and real units is correct since physical properties and body forces were incorporated in real units and the obtained results resemble the real behaviour.

The error percentage can be calculated from Equation 11.

$$\%Error = \frac{\sum_{i=1}^{n}\left(abs\left(\frac{L_{teo_i} - L_{Exp_i}}{L_{teo_i}}\right)\right)}{n} \times 100 \tag{11}$$

Where L_{teo_i} is the theoretical value, L_{Exp_i} is the experimental value, and n is the amount of values.
The error percentage was calculated for three cases: (i) FLUENT vs Experimental, (ii) LBM vs Experimental and (iii) LBM vs FLUENT. For all pairs, the second method (the one named after the 'vs') was assumed as the source of theoretical data. Table 4 shows the error percentages obtained.

Table 4: Error percentages between simulations and experimental data.

Case	FLUENT VS EXPERIMENTAL	LBM VS EXPERIMENTAL	LBM VS FLUENT
% Error	3.57	6.67	10.28

5.3. Loss Estimation

A qualitative analysis of the simulation animations and the experimental video was performed studying fluid surface topology and release time. Results show that the fluid surface topology is similar in all three cases (Figure 5); this allows inferring the following: (i) the mass amount released in each time step is similar, (ii) the orifice volumetric flow is similar and (iii) the profile of average velocity at the orifice versus time is similar.
The emptying time of the tank for different fluid head heights was also studied. The tank was considered empty when the fluid height reached half of the orifice opening. Table 5 shows the release time for LBM, FLUENT and experiments using different scenario configurations. Table 5 also shows the average released volume per unit of time (volumetric flow rate) and the error percentage between LBM and the other two methods.

Table 5: Release time in seconds for different scenario configurations.

Fluid Head/Method	Time (s)					Volumetric flow rate (cm^3/s)				
	Exp.	FLUENT	LBM	% Error (LBM-Exp.)	% Error (LBM-FLUENT)	Exp.	FLUENT	LBM	% Error (LBM-Exp.)	% Error (LBM-FLUENT)
10 cm	0.87	0.92	0.91	4.60	1.09	1149.43	1086.96	1098.90	4.40	1.10
15 cm	1.17	1.20	1.19	1.71	0.83	1282.05	1250.00	1260.50	1.68	0.84
20 cm	1.43	1.44	1.40	2.10	2.78	1398.60	1388.89	1428.57	2.14	2.86

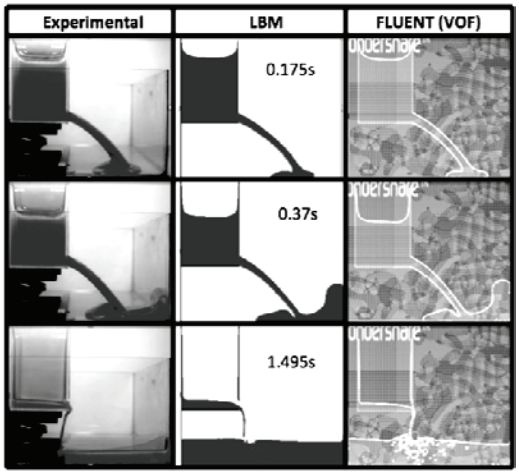

Figure 5: Animation sequence for the three studied methods.

6. Conclusions

This fast approximation has shown that non-traditional fluid dynamics approximations can correctly predict important phenomena for the process safety field, leading to useful results. Here it was shown that the LBM appropriately calculates the loss of primary containment dynamics in a tank. This statement is supported on the fact that the LBM has an error percentage under 5% for loss estimation variables when it is compared to experimental data and to results obtained from specialized software like FLUENT. For this reason the LBM is suggested as a new alternative to estimate losses and to forecast loss of containment scenarios.
Both, LBM and FLUENT, were capable of predicting correctly the studied phenomenon, although this paper has shown that LBM requires considerably less computing time than FLUENT for a simulation with the same number of elements. This makes the LBM particularly attractive for complex geometry situations that require a large number of elements, exploiting the simulation time advantage at most. Finally, this paper opens the possibility of performing LBM simulations in the process safety field not only for loss of contention scenarios, but also for dispersion events.

References

Crowl, D. & Louvar, J. F. 2002, *Chemical process safety. Fundamentals with applications,* 2nd edn, Prentice Hall International Series, Upper Saddle River.
Chang, C., Liu, C.-H. & Lin, C.-A. 2009, 'Boundary conditions for lattice Boltzmann simulations with complex geometry flows', *Computers & Mathematics with Applications,* 58**,** 940-949.
Ferziger, J. & Peric, M. 2002, *Computational Methods for Fluid Dynamics,* 3rd edn*,* Springer, Heidelberg.
He, X., Zou, Q., Luo, L.-S. & Dembo, M. 1997, 'Analytic solutions of simple flows and analysis of nonslip boundary conditions for the lattice Boltzmann BGK model', *Journal of Statistical Physics,* 87**,** 115-136.
Körner, C., Thies, M., Hofmann, T., Thürey, N. & Rüde, U. 2005, 'Lattice Boltzmann Model for Free Surface Flow for Modeling Foaming', *Journal of Statistical Physics,* 121**,** 179-196.
Lee, J. & Lee, S. 2010, 'Boundary treatment for the lattice Boltzmann method using adaptive relaxation times', *Computers & Fluids,* 39**,** 900-909.
Maier, R., Bernard, R. & Grunau, D. 1996, 'Boundary conditions for the lattice Boltzmann method', *Physics of Fluids,* 8**,** 1788-1792.
Pontiggia, M., Busini, V., Gattuso, M., Uguccioni, G. & Rota, R. 2012, 'Consequences Assessment of an Accidental Toxic Gas Release Through a CFD Tool: Effect of the Terrain and Major Obstacles', *Chemical Engineering Transactions,* 26**,** 537-542.
Skordos, P. A. 1993, 'Initial and boundary conditions for the lattice Boltzmann method', *Physical Review E,* 48**,** 4823-4842.
Succi, S. 2001, *The Lattice Boltzmann Equation for Fluid Dynamics and Beyond,* Oxford University Press, New York.
Sukop, M. C. & THRONE, D. T. 2006, *Lattice Boltzmann Modeling. An Introduction for Geoscientists and Engineers,* Springer, Heidelberg.
Thürey, N. 2007, 'Physically based Animation of Free Surface Flows with the Lattice Boltzmann Method', PhD thesis, Universtität Erlangen-Nürnberg.
Yang, Z. 2010, 'Pressure condition for lattice Boltzmann methods on domains with curved boundaries', *Computers & Mathematics with Applications,* 59**,** 2168-2177.